VDMA
Fluid Power Association

22nd ISC

International Sealing Conference

Stuttgart, Germany
October 01 - 02, 2024

Sealing Technology –
Challenges accepted!

UNI STUTTGART

© 2024 VDMA Fluidtechnik
All rights reserved. No part of this publication may be reproduced, stored in retrieval systems or transmitted in any form by any means without the prior permission of the publisher.

ISBN 978-3-8163-0768-6

Fachverband Fluidtechnik im VDMA e. V. Lyoner Str. 18
50628 Frankfurt am Main
Germany

Phone +49 69 6603-1513
E-Mail maximilian.baxmann@vdma.org
Internet www.vdma.org/fluid

Insights into the pumping behaviour of sealing counterfaces using continuous logging

Georg Haffner, Matthias Baumann, Frank Bauer

Surface structures of the sealing counterface are called “lead structures” when they have the capability to pump oil rotation dependent through the sealing contact of a rotary shaft seal systems. This feature is called “pumping effect”. The structures interrupt the equilibrium state of the sealing system, which may cause dry run or leakage as failure result. Especially for higher circumferential velocities the pumping effect increases and therefore cannot be neglected.

To assess the functional influence of lead structures on the sealing system, one can measure the pumping rate of the sealing counterface experimentally. The higher the pumping capability of a sealing counterface, the more likely the sealing system will fail. In this paper, the development a new pumping rate evaluation method with the help of a continuously measuring scale, which allows to visualize the course of the pumping rate over time, is described. With this knowledge it is possible to determine the end of the running-in phase of the rotary shaft seal and to determine the minimum duration of the pumping rate tests. The pumping rate evaluation method is demonstrated with different shaft counterfaces to validate the stability of the new method.

1 Introduction

Rotary shaft sealing systems consist of the rotary shaft seal, a fluid to be sealed and the sealing counterface [1]. The components - during operation - form a complex tribological system, which has many different external and internal influences able to affect the life expectancy of the system.

External influences are e.g. temperature, pressure, humidity or the environmental circumstances. Internal influences, on the other hand, are based on the components of the sealing system itself. The material of the rotary shaft seal (e.g. FKM or NBR), the oil (e.g. mineral oil or synthetic oil) and its compatibility with the rotary shaft seal material [2] and the sealing counterface material as well as structures on the counterface are examples of internal influences.

The sealing counterface possesses an important role in the tribological system “rotary shaft seal”. It has direct contact with the sealing lip of the rotary shaft rotary shaft seal, therefore it has to be matched to the rotary shaft seal in order to work properly. Since the sealing counterface is mostly manufactured inhouse in contrast to the rotary shaft seal which is purchase part with mostly the same tolerances and quality [3], there are different guidelines which assist the manufacturing process of the sealing counterface to match with the rotary shaft seal, e.g. [4, 5].

Those guidelines describe the material properties of the sealing counterface as well as the surface properties like roughness, maximum shape divergence and micro and macroscopic structure properties. Micro- and macroscopic structures can apply additional fluid movement through the sealing contact during operation. Such structures are called “lead”. The fluid moving, also called “pumping effect”, is rotation direction and circumferential velocity dependent.

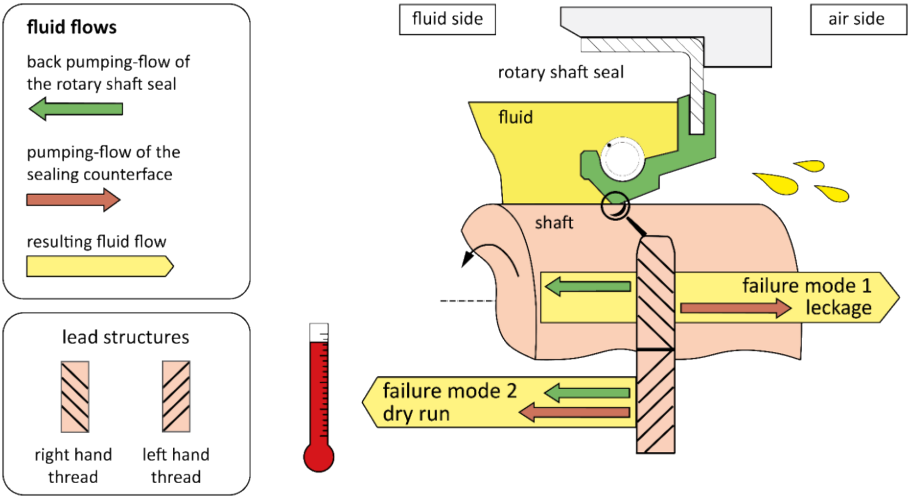

Figure 1: Failure modes due to lead

The pumping effect of the sealing counterface is mostly unwanted as it disturbs the equilibrium state of the rotary shaft seal system. A pumping effect of the sealing counterface can lead to the failure of the sealing system in two different ways, as shown in Figure 1. Either the fluid is pumped into the housing of the sealing system, so direct contact between the sealing edge and the counterface occurs with increased friction and wear which leads to thermal damage of the sealing edge and therefore leakage or the fluid is pumped out of the housing, which results in direct leakage. Both failure mechanisms result in the standstill or failure of the affected devices, expensive repairs and environmental damage.

Table 1: Categories of lead [6]

high-pass → λ_c = 20 µm → low-pass

	Category	Illustration	Classification
microscopic	micro lead	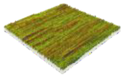	stochastically arranged, anisotropic
macroscopic	micro waviness	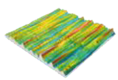	stochastically arranged, aperiodic, isotropic / anisotropic
macroscopic	macro lead	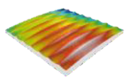	axial periodic, circumferential
any size	scratches	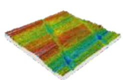	defects, any size

As mentioned before, lead can occur in different scales. Table 1 gives an overview of the lead types, their respective classification and analysis method.

Basically, lead is categorized by its scale. Measuring lead requires special hardware like a microscope with different magnifications. While scratches may appear in every scale from visible by eye to visible by microscope, the evaluation of macro- and micro lead is primarily carried out with the help of a topography measuring device (periodic/aperiodic macro lead and micro lead) or tactile measuring device (periodic macro lead).

A lot of research has been carried out to measure and evaluate lead [4, 6, 7]; it's possible to evaluate if the shaft surface should be used in a rotary shaft sealing system. But the decision is solely based on if lead is present in any of the mentioned methods. The quantitative influence of lead – e.g. how much lead is tolerable for the reliable usage – is mostly unknown.

Lead is a major influence to the equilibrium state of the sealing system; therefore, its effect is examined in pumping rate measurement runs. There are different methods for evaluating the pumping rate of a sealing system, which either check a very short time span of the pumping rate like [8], where oil rise due to pressure difference in a riser pipe is evaluated or one only checks the start and the end of the run [9, 10], which averages out the pumping rate and describes the behaviour less detailed.

The aim of this paper is to give insights in the behaviour of the sealing system during multiple runs of [10] to see the behaviour of the run-in phase of the rotary shaft seal and the development of the pumping rate over time using “lead free” sealing counterfaces and mostly same test circumstances. This is achieved using a continuous measuring scale, which is triggered using a microcontroller.

2 Materials and methods

The next section covers the used test equipment, especially the test-rig as well as the scale, the measurement procedure and the scope of the experiment of this paper.

2.1 Research approach

To investigate the pumping behaviour of a rotary shaft sealing system, a test-rig with precise geometric tolerances as well as precisely adjustable temperature and rotation speed is used. These parameters reduce the influence of clamping errors or errors due to material and fluid property changes. Furthermore, a precise scale adapted to geometric constraints of a test-rig was developed and applied, which can be read out automatically so the generated data can be visualized and evaluated algorithmically.

2.2 Test-rig

For the examinations, the modular 24 chamber test-rig [11] from the institute is used. It offers the advantage of a directly visible sealing contact, easy adjustment of the running track and good clearance underneath the test chamber, as seen in Figure 2, where the scale and a beaker are positioned.

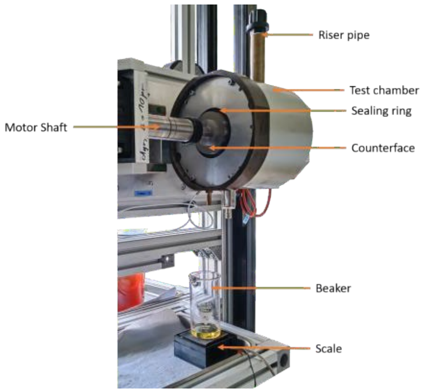

Figure 2: Test setup

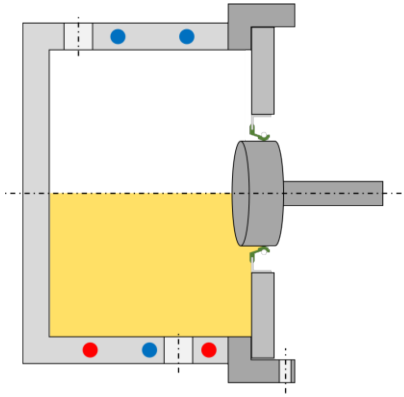

Figure 3: Cross-section of a test chamber

Every test chamber has multiple bores with heating elements (red) and bores for cooling water (blue), Figure 3. The fully assembled test setup consists of the chamber with a filtering riser pipe, so the chamber is vented and has ambience pressure, a mounted sealing counterface, and a holder for the rotary shaft seal. In front of the holder is a small outlet, which allows leakage to be collected and dropped into a beaker. The beaker itself is positioned on a scale.

Velocity, temperature of the oil sump and the load collective of every module can be controlled individually. They can be adjusted in the graphical user interface of the test-rig.

2.3 Pumping rate measurement

The pumping rate measurement is carried out after the method proposed by [9], where the rotary shaft seal is mounted in inverse direction, so the front is constantly in contact with the oil. Therefore, the rotary shaft seal will pump out oil during rotation independently of the rotation direction and the sealing counterface depending on its rotation direction.

The pumping rate of the rotary shaft seal can be calculated as followed:

$$PR_{Sealing} = \frac{1}{\Delta t} \cdot \frac{Leakage_{ccw} + Leakage_{cw}}{2} \tag{1}$$

The pumping rate of the sealing counterface can be calculated as followed:

$$PR_{Counterface} = \frac{1}{\Delta t} \cdot \frac{Leakage_{ccw} - Leakage_{cw}}{2} \tag{2}$$

In this investigation, only the pumping rate of the sealing counterface is considered. The pumping rate is calculated for every clockwise (cw)/counter clockwise (ccw) run under the limitations proposed by [9].

2.4 Continuous measuring scale

A scale was developed to continuously record the pumping behaviour of the sealing system, Figure 4. This was necessary due to the space restrictions under the test rig as well the integration into the test-rig software. The scale was extensively tested and problems such as temperature dependency were compensated for with mathematical models.

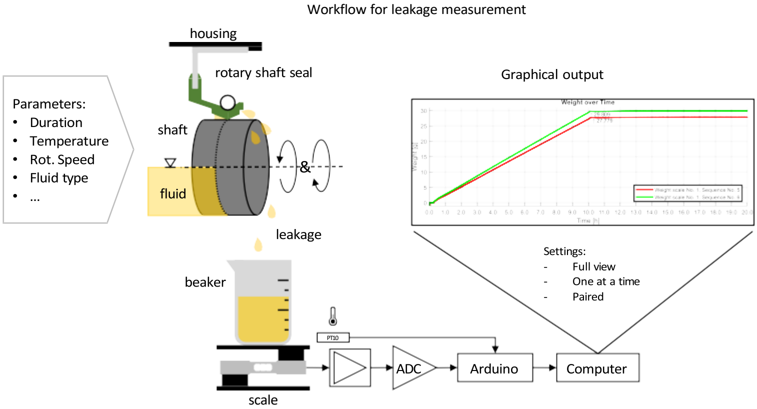

Figure 4: Schematic principle for measurement

The scale is based on a 1kg measuring range bending beam with a strain gauge full bridge. Its analogue signal is interpreted by a 24-bit analogue-digital converter, resulting in approx. 0.1 mg[1] resolution. The digital signal is processed by an Arduino alongside the signal of the device temperature, which is measured using a PT10, which is digitalized with 12-bit. The sensor is needed for the temperature compensation of the scale.

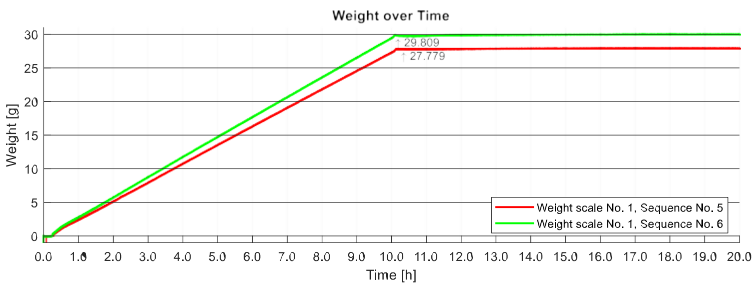

Figure 5: Continuous weight recording (cw and ccw) of a lead-free shaft surface

1 Assuming 1 bit is quantification noise

Both signals are sent to a computer over the serial interface using Python (Version 3.9). Every temperature and weight signal are saved in a text file with its proper timestamp, the measuring frequency is set to 1 s. The text file is interpreted, processed and visualized using MATLAB (Version R2022a), Figure 5.

The processing includes removal of spikes, the above-mentioned temperature compensation, offset removal to compensate the beaker weight and the division into sequences. The measurement in the upper example was carried out on a lead-free surface. The clockwise run (or odd sequence number) is coloured red, the counter clockwise run is coloured green. On the abscissa the time is applied, on the ordinate the weight. The peak weight at around the 10 h mark is also printed in the graph. The legend on the bottom-right tells which scale is used and which run (or sequence) the graph is currently displayed with its associated colour.

2.5 Scope of experiment

The test runs were carried out on two different chambers of the test-rig. Every chamber had one scale, both scales were connected to the same Arduino which received both weight signals at the same time. Both beakers were measured before and after each test-run. The measured oil was poured back into the test chamber after every test run.

The test run conditions can be taken from the following table:

Table 2: Test run conditions

Rotary shaft seal	*Freudenberg BAUM5X7 FKM*
Oil	*FVA3 mineral oil [12]*
Oil amount	*Centre of shaft*
Oil sump temperature	*80°C*
Rotational speed	*±1000 1/min*
Shaft diameter	*80 mm*
Run duration	*10 h (single direction)*
Pressure	*Ambient pressure (vented test chamber)*

The runs were carried out on different shaft surfaces, two lead-free and two macro lead-afflicted shaft surfaces. In the following overview, the topography measurements of the shaft surfaces can be seen along with their macro lead parameters, measured and evaluated according to [4]:

Table 3: Overview of selected shafts surfaces

Name	***Topography***	***Type***	***Dt [µm]***	***Dy [°]***	***DP [mm]***
LF01	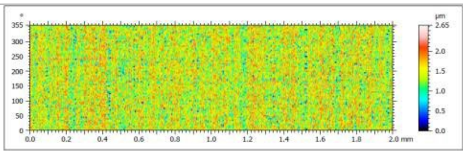	Lead-free	0.18	0.00	0.209
LF02	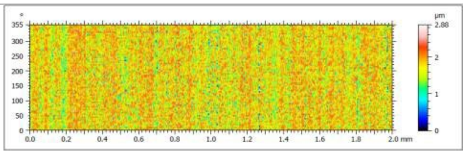	Lead-free	0.15	0.00	0.205
LA01	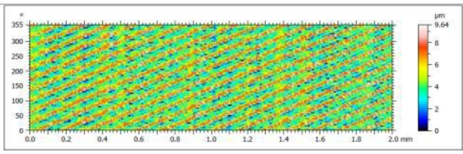	Lead-afflicted	5.10	- 0.316	0.139
LA02	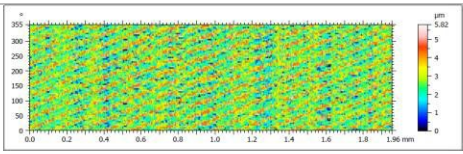	Lead-afflicted	2.34	- 0.327	0.143

The height of the topographies in Table 3 is displayed in false colour representation, where blue represents a low and red a high height value. The scaling of every surface is different to better visualize the different structures on the shaft counterfaces. Both lead-free surfaces are very similar in every mentioned macro lead parameter. A major difference in the lead-afflicted surfaces is the lead depth *Dt*, which differs about 2 times. The other two macro lead parameters, period length *DP* and lead angle *Dy*, differ significantly less. Micro lead measurement and evaluation on all shaft surface has also been carried out according to [13]; all surfaces are micro lead-free.

The test runs were carried out on the same tracks, repetitions on the lead-free shaft surfaces were carried out on a different track. This ensures the same initial condition for every sealing system.

In total, 6 runs over 180 h of test time with two lead-free and two lead afflicted surfaces were carried with continuous measurement.

3 Experimental results

The experimental results are split in two parts. First, a complete test run is evaluated and specific features and occurrences are pointed out. In the second part, the first run of the same lead-free shaft surface is considered in more detail, especially at start and the end of a run.

3.1 Continuous measurements

The continuous measurement displays the whole test period, with every clockwise and counter-clockwise run as well as the standstill time. An example of a continuous test run is seen in the following figure:

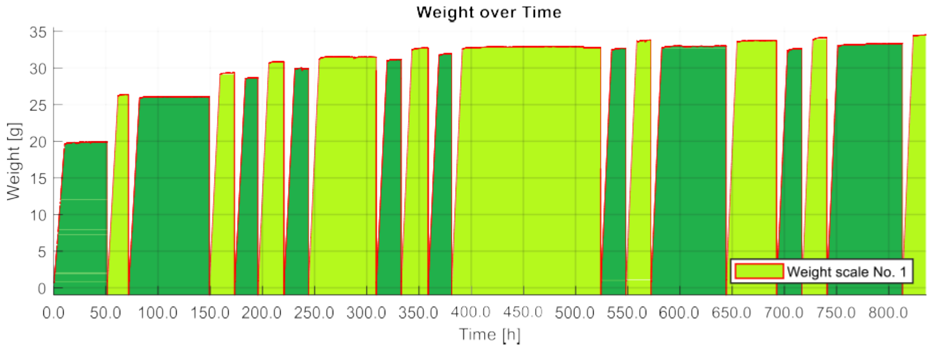

Figure 6: Full test run, LF01

Figure 6 shows 20 runs of the same sealing system using LF01 as sealing counter-face; the runs were carried out according to Table 2, clockwise runs are coloured dark green and counter clockwise runs are coloured light green. The scale is continuously acquiring weight data, after 10 hours of continuous weight rising due to rotation of the shaft, the shaft stops rotating and the weight remains at its last value since no more fluid is pumped. The different holding times after every weight rise are due to weekends or holidays. Before changing the rotational direction, the beaker is then emptied back into the test chamber to keep the fluid level at the centre of the shaft. This process is visible in the drop of the weight to below 0 g. When the beaker is put back onto the scale, the weight settles back at approx. 0 g. Afterwards, the test run is started again with the opposite rotation direction.

A clear trend is visible since the difference between the cw weight and associated ccw weight is getting continuously smaller. The difference is more apparent when looking at the fluid pumped of each cw/ccw pair and note the resulting weights, seen in Figure 7:

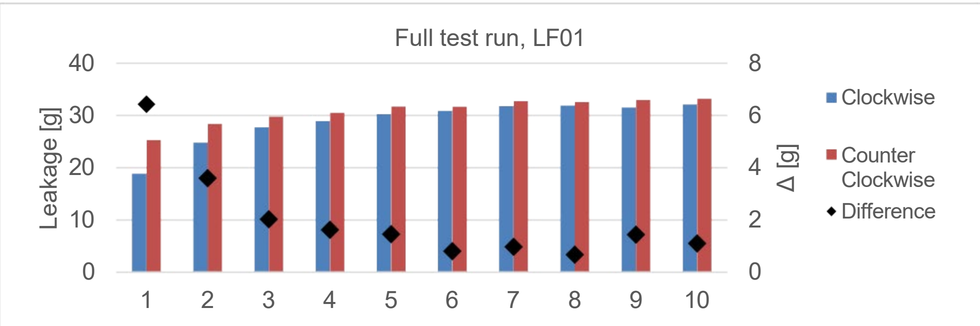

Figure 7: Weights of the full test run, LF01

The maximum weight value of every run in Figure 6 was evaluated and presented as bars in the figure above and the difference between cw and associated ccw run was positioned between both runs in a diamond shape.

The sum of the pumped fluid rises every cw/ccw run, beginning at 19 g/25 g and ending at about 32 g/33 g. But the difference between cw and ccw decreases from 6.4 g to 1.10 g, Table 4. From pair 5 to pair 10, the difference settles at about 1.15 g ± 0.35 g.

Table 4: Leakage values full test run, LF01

Pair:	1/2	3/4	5/6	7/8	9/10	11/12	13/14	15/16	17/18	19/20
cw [g]:	18,90	24,84	27,78	28,95	30,28	30,92	31,81	31,94	31,58	32,15
ccw [g]:	25,33	28,44	29,81	30,57	31,74	31,73	32,78	32,61	33,02	33,25
Δ [g]:	6,43	3,60	2,03	1,62	1,46	0,81	0,97	0,67	1,44	1,10

When assuming, this result is the final pumping rate of the sealing system in this configuration, a longer testing period for a sealing system is needed to achieve more stable results since the difference in the first cw/ccw run is more than 6 times larger compared against the last pair in the test period. The difference becomes less significant after the second and third test run. The most stable result can be achieved after the fifth cw/ccw pair, since from there on until the end of the investigation, the change pumping rate is less significant, seen in the next figure:

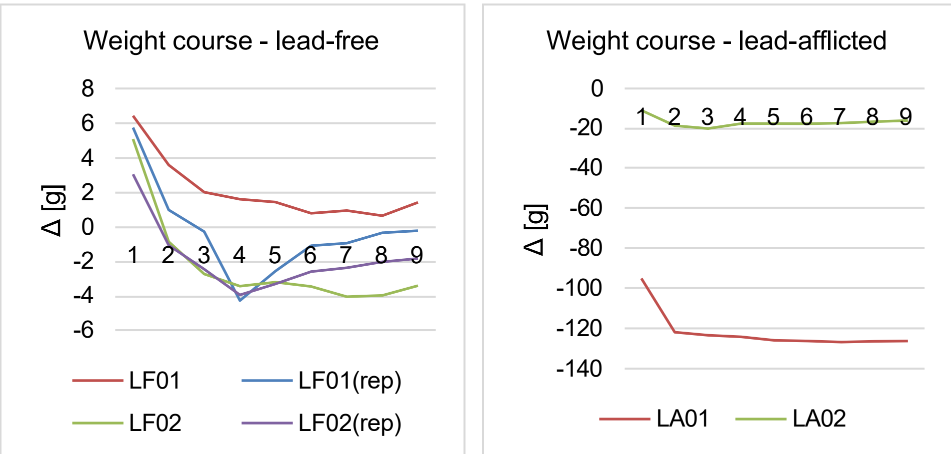

Figure 8: Weight courses

The runs were split into two diagrams since the absolute pumping rate difference between lead-free and lead-afflicted surfaces in the observation is up 60 times. All lead-free surfaces settle at about -4 g to 2 g, where the lead-afflicted surfaces spread between -120 g to -20 g. The drop in *LF01(rep)* during the 4th cw/ccw run occurred when not keeping the minimum of 10h resting time. Interestingly, the sealing system slowly rises back to about 0 g pumping rate difference, which was the last pumping rate difference seen at the 3rd cw/ccw pair.

3.2 Detailed view of a cw/ccw pair

The overview in Figure 6 gives a good insight into the pumping behaviour of a sealing system over time. The change in the difference in the pumped fluid can be observed with lead-free and lead-afflicted shaft surfaces. Next, it is interesting to see, how the sealing system itself behaves in one cw/ccw pair. Therefore, the first pair is observed in more detail since this pair showed the greatest change over the time. The cw/ccw pair is visualized in Figure 9. Both runs were put in the same diagram, with the same time scaling and the same height scaling.

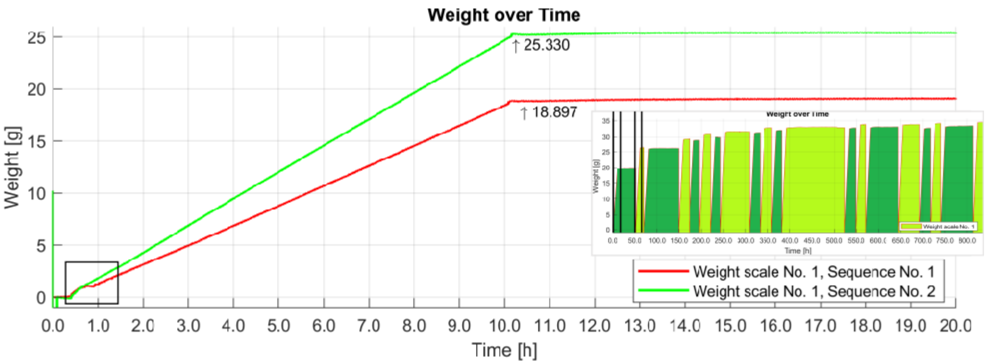

Figure 9: First run LF01, detailed view

The figure shows a section from the test-run LF01, the cw run is coloured red and ccw run is coloured green. The first run appears to have an elevation, highlighted in the grey box which disappears after about 1h of test run time. At similar position, an elevation has appeared on four of the other detailed measurement runs, but the shape of the elevation differs, Figure 10. The exceptions are LF02 and LA01, which do not appear to have an elevation in their first run.

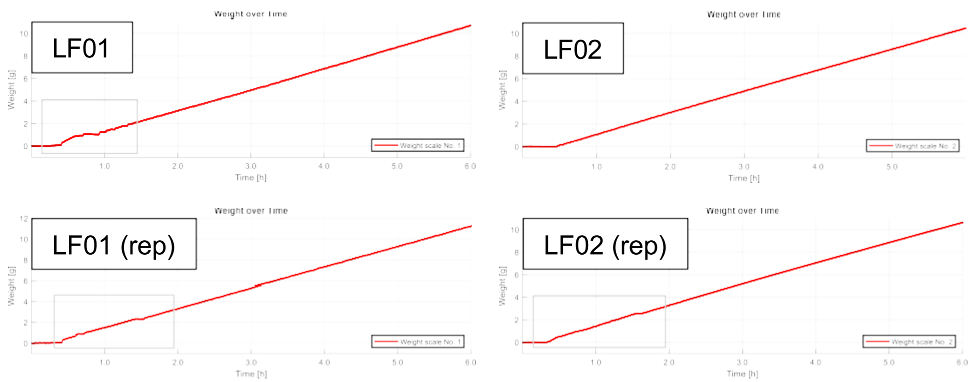

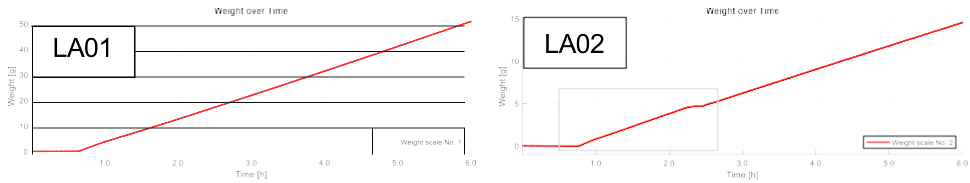

Figure 10: Initial elevation during first run

In the ccw run, an elevation cannot be seen. This might be due to the run-in behaviour of the rotary shaft seal. Based on the test-rig design, in the first minutes of the test run, no leakage is detected because the fluid first collects at the sealing lip before it combines to a droplet and falls into the beaker. The next droplets are more uniform and easier to discover as seen in the magnification view of hour 2 and hour 4.

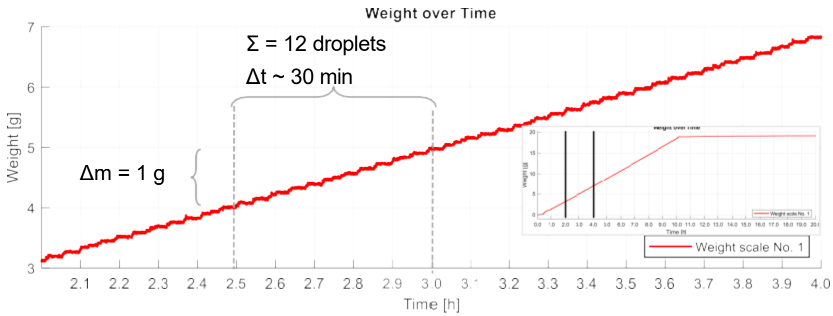

Figure 11: Weight course LF01, 2h-4h

The resolution of the scale is sufficient enough to represent a droplet and approximate weight and the duration between every droplet, which then can be evaluated. In Figure 11, a droplet has the approximate weight of 0.083 g and appears every 2.5 minutes. Accumulated over the test duration, the final weight of the pumped oil is 19.92 g, which matches well with the measured leakage (18.90 g) when not considering the run-in phase. This means after the run-in phase. the pumping rate behaviour remains mostly linear over the testing time of the run.

At the end of each run, no more fluid is pumped and the fluid around the sealing edge is no longer dragged along the circumference of the sealing edge.

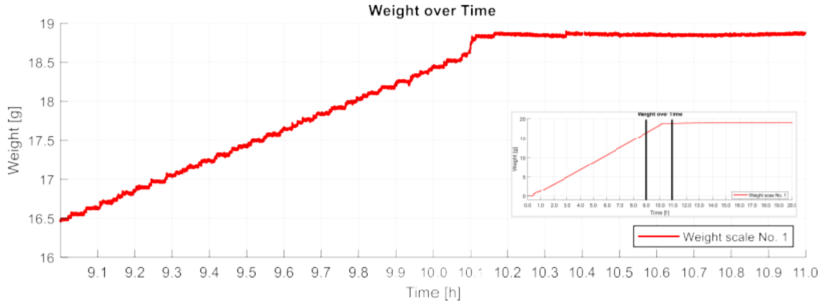

Figure 12: Detailed view of the end of a run, LF01

The fluid collects at the lowest point of the sealing edge, forms into a droplet and runs down into the beaker. This behaviour can be seen in Figure 12. The offset of 0.1 hours to the 10 h mark is the result of the scale being switched on first before the test run is started. At the 10.1 h mark, a bigger than usual droplet with about 0.25 g (compared to ~0.09 g) was formed and dropped into the beaker. Afterwards, at standstill of the test-rig, near 10.2 h and near 10.4 h, a small droplet can also be seen.

3.3 Visual examination of components

A change in the rate of pumped fluid of every sealing system has been determined, Figure 8. Such an effect can appear due to changes in the sealing system components like the rotary shaft seal or the sealing counterface. Both components are visually examined using a digital microscope.

3.3.1 Visual examination of rotary shaft seal

The sealing edge is a highly stressed part of the rotary shaft seal. Wear as well as thermal damage may appear when the sealing system isn't proper designed. To assess the condition of the sealing edge, direct view onto the sealing edge is needed. It was achieved using [14]; the condition of rotary shaft seal of LF01 compared to a new rotary shaft seal is displayed in Figure 13:

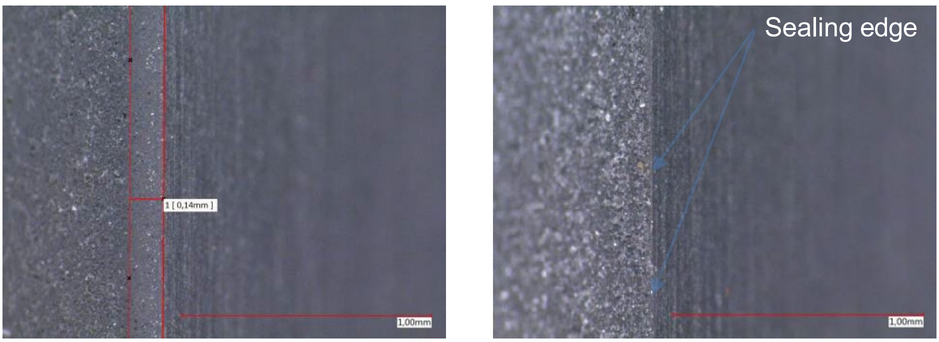

Figure 13: Comparison of used vs. new sealing edge

The sealing edge is not discoloured, so no thermal damage occurred on the sealing edge. The sealing contact was continuously supplied with fresh oil. Compared to a new sealing edge of the same batch (Figure 13, image on the right), wear can definitely be seen. The sealing edge, even though constantly supplied with oil, still wears out, meaning, the contact is not constantly fully lubricated. It has an approximate wear width of about 0.14 mm where the new sealing edge is still “sharp”.

The wear width of the sealing edges of the other (lead-free surface) rotary shaft seals also settle around 0.14 mm to 0.18 mm. Since all rotary shaft seals appear to have wear on the sealing edges, which is similar over the test runs, the formation of wear during the runs can explain the behaviour of the pumped fluid, determined in 3.1. Starting with the first run pair, the difference between cw and ccw run is 6.43 g, the absolute fluid pumped is around 19 g (cw) and 25 g (ccw). The difference in the following run pair (3/4) in fluid pumped is only 3.6 g, so it can be assumed, that wear on the sealing edge was already formed during the first run pair (1/2). With each successive run pair, the rate of change in the difference of the pumped fluid becomes smaller indicating a decrease in wear formation and a stabilisation of the tribological state in the sealing contact. At the fifth run pair of LF01, the change of fluid pumped (30 g/32 g) and the difference between the run is not changing as significantly compared to the first run pair. At this point in this investigation it can be assumed that the sealing edge did not wear significantly further.

3.3.2 Visual examination of sealing counterface

A change in the surface of the sealing counterface can also cause the change of the pumping rate behaviour. In visual microscopy, the deeper a grove, the darker the colour gets. The surfaces do not have a groove with a high wear depth, since only light colour changes can be seen. On the surfaces, it’s only possible to see the running track of the rotary shaft seal, Figure 14:

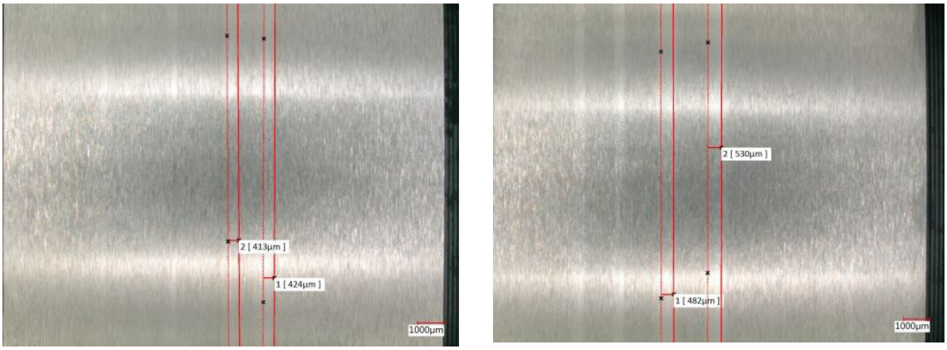

Figure 14: Surface analysis LF01(left) and LF02 (right)

The running tracks are hardly visible in the magnified view on the sealing counterface. Both images were taken with 50x magnification and the same light settings. The peaks of the roughness of the surfaces have been smoothed out but no measurable depth has been created during the test runs. The smoothing of the peaks of the roughness cannot explain the behavior seen in 3.1, since the major macroscopic structures would still be completely intact.

4 Discussion and conclusion

The paper presented a more detailed view into the pumping behaviour of different shaft surfaces with the help of continuous measuring scales during pumping rate measurements according to [9, 10]. The goal was to visualize the running-in phase of the sealing and derive a more stable duration for pumping rate measurements. Using a continuous measuring scale proved to be a convenient way to carry out pumping rate measurements since the weight difference can be calculated automatically and the beaker isn't needed to be weighed before and after each run.

As seen in the overview images in Figure 8, the first pumping rate differs in absolute value and can also differ in sign compared to the following pumping rate measurements. In the scope of this paper, it is recommended to use a at least 6 measurement runs, three clockwise and three counter-clockwise to achieve a more stable result for the pumping rate since the scattering of the leakage is smaller. Longer testing periods result in a more stable pumping rate. The change in pumped fluid can be traced back to the wear of the sealing edge although it was constantly surrounded by oil. A closer examination of the sealing counterfaces hasn't given indication of the change of pumped fluid, since only smoothening of roughness tips was seen.

After 180 hours of testing according to Table 2, the difference between the cw and corresponding ccw run settles at about 1.15 g ± 0.35 g. Since a deviation is still present, a much longer testing time could be used to check, where the sealing system with the corresponding shaft surface settles.

When looking at the first run of a sealing system in more detail, an elevation can be captured, where the pumping rate deviates from a constant increase. This different behaviour finishes after about 2-3 h of continuous running. In two of six runs on two different test chambers, this effect hasn't appeared, which argues against a system-wide effect. The duration and magnitude of the elevation are also not constant. There, more runs with continuous measuring scales could be carried out systematically in order to understand how this elevation appears.

The method allows further applications such as leakage detection or extensive comparison of sealing systems. It's also possible to implement the scales into an existing test rig software to allow more data of the test run to be collected.

5 Nomenclature

Variable	***Description***	***Unit***
cw	clockwise	[-]
ccw	counter clockwise	[-]
Dy	Lead angle	[°]

DP	Period length	[mm]
Dt	Lead depth	[µm]
Δt	Run duration	[h]
$Leakage_{cw}$	Mass of pumped fluid during cw operation	[g]
$Leakage_{ccw}$	Mass of pumped fluid during ccw operation	[g]
$PR_{Sealing}$	Pumping Rate of a radial shaft seal	{g/h]
$PR_{Counterface}$	Pumping Rate of a sealing counterface	[g/h]

6 Authors

University of Stuttgart, Institute of Machine Components (IMA)

Pfaffenwaldring 9, 70569 Stuttgart, Germany:

Georg Haffner, M. Sc., ORCID 0000-0002-6484-235X, georg.haffner@ima.uni-stuttgart.de

Dr.-Ing. Matthias Baumann, ORCID 0000-0002-1962-5153, matthias.baumann@ima.uni-stuttgart.de

Apl. Prof. Dr.-Ing. Frank Bauer, ORCID 0000-0001-7799-7628, frank.bauer@ima.uni-stuttgart.de

7 Literaturverzeichnis:

[1] **Bauer, F.:** *Federvorgespannte-Elastomer-Radial-Wellendichtungen. Grundlagen der Tribologie & Dichtungstechnik, Funktion und Schadensanalyse*, Wiesbaden, Heidelberg: Springer Vieweg, 2021, Springer Fachmedien Wiesbaden, - ISBN 978-3-658-32922-8.

[2] **Florez, A.; Hentschke, C.; Jacobs, G.:** *Elastomerverträglichkeit. Verträglichkeit von Schmierstoffen und Elastomeren*. Abschlussbericht FVA Vorhaben Nr. 683 I, IGF-Nr. 17450 N, Frankfurt am Main: FVA, 2015, Forschungsvereinigung Antriebstechnik e.V. (FVA).

[3] **Deutsches Institut für Normung e.V.:** DIN 3761-1: *Radial-Wellendichtringe für Kraftfahrzeuge - Begriffe; Maßbuchstaben; zulässige Abweichungen; Radialkraft*, Berlin: Beuth. Januar 1984.

[4] **Mercedes-Benz:** Norm MBN 31007-7: *Geometrische Produktspezifikationen (GPS) - Oberflächenbeschaffenheit Mess- und Auswerteverfahren zur Bewertung von drallreduzierten dynamischen Dichtflächen.* September 2008.

[5] **Deutsches Institut für Normung e.V.:** DIN 3760: *Radial-Wellendichtringe*, Berlin. September 1996.

[6] **Baumann, M.:** *Abdichtung drallbehafteter Dichtungsgegenlaufflächen - Messung, Analyse, Bewertung und Grenzen*. Dissertation, 2017, Universität Stuttgart, Institut für Maschinenelemente, - ISBN 978-3-936100-69-3.

[7] **Engelfried, M.; Baumann, M.; Bauer, F.:** *3D-Makrodrall - Strukturbasierte 3D-Analyse von Makrodrall*. Forschungsheft 1471, Forschungsvereinigung Antriebstechnik e.V., Abschlussbericht FVA Vorhaben Nr. 876 I, Frankfurt am Main, 2022.

[8] **Britz, S.:** *Ein Beitrag zur Erfassung der Funktionsprinzipien dynamischer Wellendichtungen unter besonderer Berücksichtigung des Radialwellendichtrings*. Dissertation, 1988, Universität Kaiserslautern.

[9] **Raab, H.:** *Wellenlaufflächen. Einfluß der Wellenlauffläche auf das Dichtverhalten von Radial-Wellendichtringen*. Abschlussbericht FKM Vorhaben Nr. 211, AiF-Nr. 10670, Frankfurt am Main: FKM, 1998, Forschungskuratorium Maschinenbau e.V. (FKM).

[10] **Kawahara, Y.; Hirabayashi, H.:** *A Study of Sealing Phenomena on Oil Seals*. A S L E Transactions. 1979, 22 (1), S. 46–55.

[11] **Universität Stuttgart, Institut für Maschinenelemente:** *Wellendichtungen 24-Zellen-Dauerprüfstand.* Universität Stuttgart, Institut für Maschinenelemente (Hrsg.), IMA-TechSheet, V1, #101010, Stuttgart, URL: https://www.ima.uni-stuttgart.de/dokumente/forschung/dichtungstechnik/einrichtungen/101010.pdf.

[12] *Referenzöle: Referenzöle für Wälz- und Gleitlager-, Zahnrad- und Kupplungsversuche. Datensammlung für Mineralöle*, Frankfurt am Main: FVA, 1985, Forschungsvereinigung Antriebstechnik e.V. (FVA).

[13] **Universität Stuttgart, Institut für Maschinenelemente:** *IMA-Mikrodrall®Analyse.* Universität Stuttgart, Institut für Maschinenelemente (Hrsg.), IMA-TechSheet, V1, #104140, Stuttgart, URL: https://www.ima.uni-stuttgart.de/dokumente/forschung/dichtungstechnik/dienstleistungen/104140.pdf.

[14] **Universität Stuttgart, Institut für Maschinenelemente:** *IMA-Sealobserver.* Universität Stuttgart, Institut für Maschinenelemente (Hrsg.), IMA-TechSheet, V1, #102070, Stuttgart, URL: https://www.ima.uni-stuttgart.de/dokumente/forschung/dichtungstechnik/einrichtungen/102070.pdf.

https://doi.org/10.61319/DI2CJQ5C